MING QIU ZHANG • MIN ZHI RONG

EXTRINSIC AND INTRINSIC APPROACHES TO SELF-HEALING POLYMERS AND POLYMER COMPOSITES

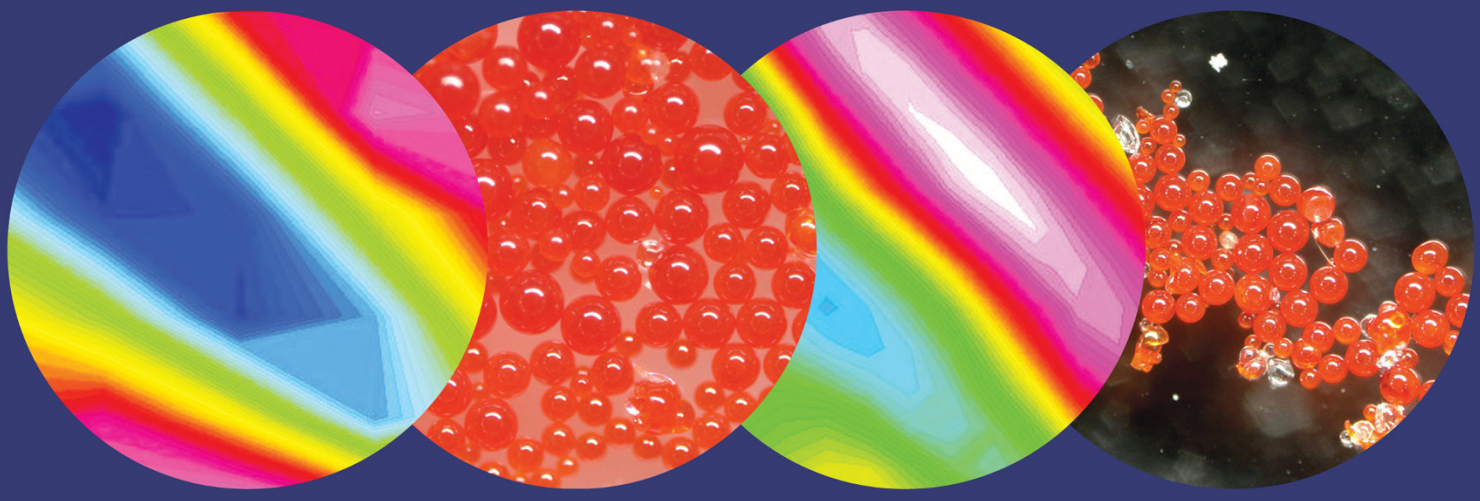

WILEY

Extrinsic and Intrinsic Approaches to Self-Healing Polymers and Polymer Composites

Extrinsic and Intrinsic Approaches to Self-Healing Polymers and Polymer Composites

Ming Qiu Zhang and Min Zhi Rong

Materials Science Institute, Zhongshan University
Guangzhou, China

WILEY

This edition first published 2022

Registered Office
John Wiley & Sons, Inc., 111 River Street, Hoboken, NJ 07030, USA

Editorial Office
111 River Street, Hoboken, NJ 07030, USA

For details of our global editorial offices, customer services, and more information about Wiley products visit us at www.wiley.com.

Wiley also publishes its books in a variety of electronic formats and by print-on-demand. Some content that appears in standard print versions of this book may not be available in other formats.

Library of Congress Cataloging-in-Publication Data applied for

[Hardback]: 9781119629955

Cover Design: Wiley
Cover Images: courtesy of Ming Qiu Zhang. Min Zhi Rong, Dong Yu Zhu and Nan Nan Xia

Set in 9.5/12.5pt STIXTwoText by Straive, Pondicherry, India

10 9 8 7 6 5 4 3 2 1

Contents

Preface *viii*

1 Basics of Self-Healing – State of the Art *1*
1.1 Background *1*
1.1.1 Adhesive Bonding for Healing Thermosetting Materials *2*
1.1.2 Fusion Bonding for Healing Thermoplastic Materials *4*
1.1.3 Bioinspired Self-Healing *5*
1.2 Intrinsic Self-Healing *6*
1.2.1 Self-Healing Based on Reversible Covalent Chemistry *7*
1.2.1.1 Healing Based on General Reversible Covalent Reactions *7*
1.2.1.2 Healing Based on Dynamic Reversible Covalent Reactions *16*
1.2.2 Self-Healing Based on Supramolecular Interactions *22*
1.2.2.1 Coordination Bonds *22*
1.2.2.2 Ionic Associations *26*
1.2.2.3 Hydrogen Bonds *27*
1.2.2.4 Other Intermolecular Forces *29*
1.2.2.5 Host–Guest Inclusion *30*
1.3 Extrinsic Self-Healing *31*
1.3.1 Self-Healing in Terms of Healant Loaded Pipelines *31*
1.3.1.1 Hollow Tubes and Fibers *31*
1.3.1.2 Three-Dimensional Microvascular Networks *33*
1.3.2 Self-Healing in Terms of Healant Loaded Microcapsules *35*
1.3.2.1 Methods of Microencapsulation *36*
1.3.2.2 Healing Chemistries *40*
1.4 Insights for Future Work *45*
References *48*

2 Extrinsic Self-Healing via Addition Polymerization *64*
2.1 Design and Selection of Healing System *64*
2.2 Microencapsulation of Mercaptan and Epoxy by In-Situ Polymerization *66*
2.2.1 Microencapsulation of Mercaptan *66*
2.2.2 Microencapsulation of Epoxy *70*
2.3 Filling Polymeric Tubes with Mercaptan and Epoxy *73*
2.4 Characterization of Self-Healing Functionality *74*
2.4.1 Self-Healing Epoxy Materials with Embedded Dual Encapsulated Healant – Healing of Crack Due to Monotonic Fracture *74*
2.4.2 Factors Related to Performance Improvement *78*
2.4.3 Self-Healing Epoxy Materials with Embedded Dual Encapsulated Healant – Healing of Fatigue Crack *84*
2.4.4 Self-Healing Epoxy/Glass Fabric Composites with Embedded Dual Encapsulated Healant – Healing of Impact Damage *90*

2.4.5 Self-Healing Epoxy/Glass Fabric Composites with Self-Pressurized Healing System *95*
2.5 Concluding Remarks *104*
References *104*

3 Extrinsic Self-Healing Via Cationic Polymerization *108*
3.1 Thermosetting *111*
3.1.1 Microencapsulation of Epoxy by Ultraviolet Irradiation-Induced Interfacial Copolymerization *111*
3.1.2 Encapsulation of Boron-Containing Curing Agent *120*
3.1.2.1 Loading Boron-Containing Curing Agent onto Porous Media *120*
3.1.2.2 Microencapsulation of Boron-Containing Curing Agent Via the Hollow Capsules Approach *122*
3.1.3 Characterization of Self-Healing Functionality *130*
3.1.3.1 Self-Healing Epoxy Materials with Embedded Epoxy-Loaded Microcapsules and $(C_2H_5)_2O{\cdot}BF_3$-Loaded Sisal *130*
3.1.3.2 Self-Healing Epoxy Materials with Embedded Dual Encapsulated Healant *135*
3.1.4 Preparation of Silica Walled Microcapsules Containing $SbF_5{\cdot}HOC_2H_5/HOC_2H_5$ *140*
3.1.5 Self-Healing Epoxy Materials with Embedded Epoxy-Loaded Microcapsules and $SbF_5{\cdot}HOC_2H_5/HOC_2H_5$-Loaded Silica Capsules *140*
3.1.6 Preparation of Silica Walled Microcapsules Containing TfOH *146*
3.1.7 Self-Healing Epoxy Materials with Embedded Epoxy-Loaded Microcapsules and TfOH-Loaded Silica Capsules *146*
3.2 Thermoplastics *151*
3.2.1 Preparation of IBH/GMA-Loaded Microcapsules *151*
3.2.2 Self-Healing PS Composites Filled with IBH/GMA-Loaded Microcapsules and $NaBH_4$ Particles *151*
3.3 Concluding Remarks *155*
References *156*

4 Extrinsic Self-Healing via Anionic Polymerization *159*
4.1 Preparation of Epoxy-Loaded Microcapsules and Latent Hardener *160*
4.1.1 Microencapsulation of Epoxy by In-Situ Condensation *160*
4.1.2 Preparation of Imidazole Latent Hardener *162*
4.2 Self-Healing Epoxy Materials with Embedded Epoxy-Loaded Microcapsules and Latent Hardener *164*
4.3 Self-Healing Epoxy/Woven Glass Fabric Composites with Embedded Epoxy-Loaded Microcapsules and Latent Hardener – Healing of Interlaminar Failure *167*
4.4 Durability of Healing Ability *174*
4.5 Self-Healing Epoxy/Woven Glass Fabric Composites with Embedded Epoxy-Loaded Microcapsules and Latent Hardener – Healing of Impact Damage *178*
4.6 Concluding Remarks *185*
References *185*

5 Extrinsic Self-Healing Via Miscellaneous Reactions *189*
5.1 Extrinsic Self-Healing Via Nucleophilic Addition and Ring-Opening Reactions *190*
5.1.1 Microencapsulation of GMA by In-Situ Polymerization *190*
5.1.2 Self-Healing Epoxy Materials with Embedded Single-Component Healant *194*
5.2 Extrinsic Self-Healing Via Living Polymerization *200*
5.2.1 Preparation of Living PMMA and Its Composites with GMA-Loaded Microcapsules *201*
5.2.2 Self-Healing Performance of Living PMMA Composites Filled with GMA-Loaded Microcapsules *202*
5.2.3 Preparation of GMA-Loaded Multilayered Microcapsules and their PS-Based Composites *208*
5.2.4 Self-Healing Performance of PS Composites Filled with GMA-Loaded Multilayered Microcapsules *210*
5.3 Extrinsic Self-Healing Via Free Radical Polymerization *215*
5.3.1 Microencapsulation of Styrene and BPO *215*
5.3.2 Self-Healing Performance of Epoxy Composites Filled with Dual Capsules *218*
5.4 Concluding Remarks *220*
References *221*

6 Intrinsic Self-Healing Via the Diels–Alder Reaction *223*
6.1 Molecular Design and Synthesis *225*
6.1.1 Synthesis of DGFA *226*
6.1.2 Reversibility of DA Bonds and Crack Remendability of DGFA-Based Polymer *228*
6.1.3 Synthesis and Characterization of FGE *234*
6.1.4 Reversibility of DA Bonds and Crack Remendability of FGE-Based Polymer *236*
6.2 Blends of DGFA and FGE *240*
6.2.1 Reversibility of DA Bonds *241*
6.2.2 Crack Remendability of Cured DGFA/FGE Blends *244*
6.3 Concluding Remarks *247*
References *248*

7 Intrinsic Self-Healing Via Synchronous Fission/Radical Recombination of the C—ON Bond *250*
7.1 Thermal Reversibility of Alkoxyamine in Polymer Solids *251*
7.2 Self-Healing Cross-linked Polystyrene *258*
7.2.1 Synthesis *258*
7.2.2 Characterization *259*
7.3 Self-Healing Epoxy *263*
7.3.1 Synthesis *264*
7.3.2 Characterization *265*
7.4 Self-Healing Polymers Containing Alkoxyamine with Oxygen Insensitivity and Reduced Homolysis Temperature *270*
7.4.1 Synthesis *272*
7.4.2 Characterization *272*
7.5 Reversible Shape Memory Polyurethane Network with Intrinsic Self-Healability of Wider Crack *277*
7.5.1 Synthesis *278*
7.5.2 Characterization *280*
7.6 Concluding Remarks *285*
References *285*

8 Intrinsic Self-Healing Via Exchange Reaction of the Disulfide Bond *288*
8.1 Room-Temperature Self-Healable and Remoldable Cross-Linked Polysulfide *288*
8.2 Sunlight Driven Self-Healing Cross-Linked Polyurethane Containing the Disulfide Bond *297*
8.2.1 Cross-Linked Polyurethane *297*
8.2.1.1 Bulk Polymer *297*
8.2.1.2 Composites with Silver Nanowires as Strain Sensor *302*
8.2.2 Commercial Silicone Elastomer *309*
8.3 Self-Healing and Reclaiming of Vulcanized Rubber *317*
8.4 Concluding Remarks *326*
References *328*

Index *332*

Preface

The global study of self-healing polymers and polymer composites started roughly at the beginning of this century based on the consensus that it represents a next-generation technology, which would greatly improve the performance of products, including, but not limited to, their reliability and durability. Two decades have past since then. When summarizing the present status, we find there has not yet been a landmark example of a commercial application. It turns out that our prediction of the development of the newly emerging innovation made in our book *Self-Healing Polymers and Polymer Composites*, which was published by Wiley in 2011, was too optimistic. Nowadays, scientists are still working hard in both theoretical and applied research. In this context, an updated book is necessary to reflect the latest achievements, which fits with the vigor and vitality of the study activities.

Being involved in the early stage of the research, we witnessed the evolution track of the movement. In general, the strategies of self-healing polymers and polymer composites are classified into two categories: extrinsic and intrinsic. The former makes use of the healing vessels (e.g. microcapsules, micropipelines, and vascular networks) embedded in the target materials to be repaired, which would be broken upon damaging the materials, releasing fluidic healing agent to the cracked sites and rebinding the cracks via chemical/physical interactions across the interface. In contrast, the latter operates by means of reversible intra- and/or intermacromolecular interactions, and no additional healing agent is required. A few groups investigated intrinsic self-healing of polymers as early as the 1970s from the angle of polymer physics. Entanglement of molecular chains acted as the main mechanism of wound healing. In 2001, Professor Scott White and his coworkers at the University of Illinois at Urbana-Champaign published a paper about self-healing in terms of healing capsules. Afterwards, extrinsic self-healing attracted plenty of research interest worldwide. In the meantime, intrinsic self-healing via chemical reversible covalent and noncovalent interactions grew so fast that it was ahead of extrinsic self-healing once again with respect to the materials species and properties to be restored. Nevertheless, chemistry has made a greater contribution this time, as more and more chemists have become involved, focusing on molecular design and synthesis as well as functionalities recovery. Intrinsic self-healing ability has been a standard feature of materials in some cases. In addition, the development of intrinsic self-healing has created other new accompanying techniques, such as reprocessing, reshaping and recycling, topology rearrangement, and processing difficult-to-process materials of traditionally nonreworkable thermosetting polymers. The new possibilities go beyond the scope of classic polymer engineering and enrich the measures of material diversification.

The style of writing and organization of our abovementioned book is followed herein, so that this book will provide the reader with an overall view of the ongoing research, and more importantly, inspiration for the development of novel materials and functionalities.

Chapter 1 serves as an introduction to the field of self-healing polymers and polymer composites. In addition to the general scope, the achievements made by different laboratories are carefully reviewed. Personal viewpoints of the authors are addressed showing the challenges, trends, and future directions. In Chapters 2–8, the self-healing strategies proposed by the authors' group are introduced, which are structured in accordance to the chemical reactions responsible for crack healing. Chapter 2 is dedicated to the healing reaction governed by addition polymerization and the self-healing systems based microcapsules and plastic tubes as well, which are able to work without manual intervention. High healing efficiency, determined by static fracture, impact and fatigue tests, is acquired for epoxy composites. To improve healing speed and widen windows of processing and operation of self-healing thermosetting materials, a few fast hardeners are introduced to work with epoxy monomer forming new groups of healing agent, as discussed in Chapter 3. Taking advantage of cationic polymerization, not only repair of cracks is

possible at and below room temperature like the epoxy-mercaptan pair, but also crack healing is greatly accelerated. Besides, redox cationic polymerization is used for healing of thermoplastics. Chapter 4 describes the self-healing polymeric materials for advanced engineering applications, driven by anionic polymerization. The healing system consists of epoxy-loaded microcapsules and imidazole latent hardener. The latter can be well pre-dissolved in an uncured composites' matrix, leading to homogenous distribution of the reagent on a molecular scale. The major concern of Chapter 5 lies in usage of small molecule monomers as healing agent instead of epoxy monomer. Accordingly, nucleophilic addition, ring-opening reaction, atom transfer radical polymerization, and free radical polymerization prove effective in rebinding the cracked planes. Unlike the extrinsic self-healing approaches surveyed in Chapters 2–5, Chapter 6 deals with design, synthesis and characterization of intrinsic self-healing epoxy, in which thermally reversible Diels–Alder bonds account for crack healing via chain reconnection. In addition to the remendability, the cured version of the novel epoxy has similar mechanical performance to conventional epoxy. In Chapter 7, the intrinsic self-healing via reversible C—ON bonds is analyzed. Because of the synchronous fission/radical recombination of C—ON bonds, the polymers containing this type of reversible covalent bond can be self-healed in a one-step fashion, which prevents material distortion during healing as for those containing Diels–Alder bonds. Lastly, Chapter 8 demonstrates the application of reversible S—S bonds in self-healing polymers. The disulfide bonds in the tailor-made polymers as well as the commercial silicone elastomer and vulcanized rubber can be triggered under the stimuli of heating and sunlight, offering satisfactory healing efficiency.

It is our intention to emphasize integration of existing techniques and/or inventing novel synthetic approaches for application-oriented material design and fabrication. Having gone through the book, readers would have a comprehensive knowledge of the field, while new researchers might have an idea of the framework for creating new materials or new applications. Readers from both academic and industrial communities will be provided with a grasp of the achievements to date and an insight into future developments. In addition, graduate students may be able to combine theories learnt in the classroom with practical research and development of materials. These are the goals of this book.

We would like to acknowledge support from the Natural Science Foundation of China (Grants 52 033 011, 51 773 229, 51 673 219, 51 333 008, and 51 873 235). We would also like to thank the team at John Wiley & Sons for their assistance throughout the publication process. In addition, we hope that the publisher is successful with this new book.

Guangzhou, February 2021 *Ming Qiu Zhang*
Min Zhi Rong

1

Basics of Self-Healing – State of the Art

CHAPTER MENU

1.1 Background, 1
1.1.1 Adhesive Bonding for Healing Thermosetting Materials, 2
1.1.2 Fusion Bonding for Healing Thermoplastic Materials, 4
1.1.3 Bioinspired Self-Healing, 5
1.2 Intrinsic Self-Healing, 6
1.2.1 Self-Healing Based on Reversible Covalent Chemistry, 7
1.2.1.1 Healing Based on General Reversible Covalent Reactions, 7
1.2.1.2 Healing Based on Dynamic Reversible Covalent Reactions, 16
1.2.2 Self-Healing Based on Supramolecular Interactions, 22
1.2.2.1 Coordination Bonds, 22
1.2.2.2 Ionic Associations, 26
1.2.2.3 Hydrogen Bonds, 27
1.2.2.4 Other Intermolecular Forces, 29
1.2.2.5 Host–Guest Inclusion, 30
1.3 Extrinsic Self-Healing, 31
1.3.1 Self-Healing in Terms of Healant Loaded Pipelines, 31
1.3.1.1 Hollow Tubes and Fibers, 31
1.3.1.2 Three-Dimensional Microvascular Networks, 33
1.3.2 Self-Healing in Terms of Healant Loaded Microcapsules, 35
1.3.2.1 Methods of Microencapsulation, 36
1.3.2.2 Healing Chemistries, 40
1.4 Insights for Future Work, 45
References, 48

1.1 Background

Polymers and polymer composites have been widely used in important engineering fields including aerospace, marine, automotive, surface transport, and sports equipment because of their advantages including light weight, good processibility, and chemical stability in any atmospheric conditions. However, long-term durability and reliability of polymeric materials are still problematic when they are used for structural applications [1, 2]. This is particularly true when impact resistance is concerned, which is a critical aspect of vehicle design. Their inability to undergo plastic deformation results in energy adsorption via the creation of defects and damage. Besides, exposure to a harsh environment would easily lead to degradation of polymeric components. Comparatively, microcracking or hidden damage is one of the fatal deteriorations generated either during manufacturing or in service as a result of mechanical stress or cyclic thermal fatigue (Figure 1.1). Its propagation and coalescence would bring about catastrophic failure of the materials and hence significantly shorten the lifetime of the structures.

Extrinsic and Intrinsic Approaches to Self-Healing Polymers and Polymer Composites, First Edition. Ming Qiu Zhang and Min Zhi Rong.

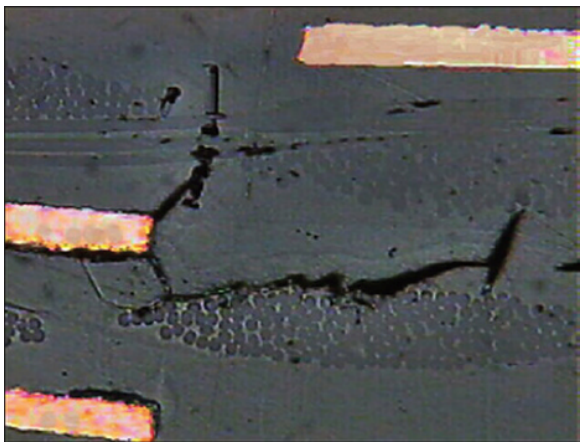

Figure 1.1 Cohesive failures beside plated through holes on copper clad laminates, which used to be produced by thermal stress.

1.1.1 Adhesive Bonding for Healing Thermosetting Materials

Damaged composites or composite structures should be repaired when significant structural degradation is detected [3]. The routine repair procedures for thermosetting composites are shown in Scheme 1.1. Some damage to composites is obvious and easily assessed but in some cases the damage may first appear quite small, although the real damage is much greater. Impact damage to a fiber can appear as a small dent on the reinforced composite surface but the underlying damage can be much more extensive. The decision to repair or scrap is determined by considering the extent of repair needed to replace the original structural performance of the composite [4]. Other considerations are the repair costs, the position and accessibility of the damage, and the availability of suitable repair materials. Easy repairs are usually small or do not affect the structural integrity of the component. Complex repairs are needed when the damage is extensive and the original structural performance of the component needs to be replaced. The best choice of materials would be to use the original fibers, fabrics, and matrix resin. Any alternative would need careful consideration of the service environment of the repaired composite, i.e. hot, wet, and mechanical performance. The proposed repair scheme should meet all the original design requirements for the structure. Some repairs need specialist equipment of a workshop and some form of improvised repair is needed to return the component to a suitable repair workshop. A temporary repair, usually in the form of a patch, can be fixed to the component. Usually a "belt and braces" approach is taken to ensure safety until the component can be repaired at a later date.

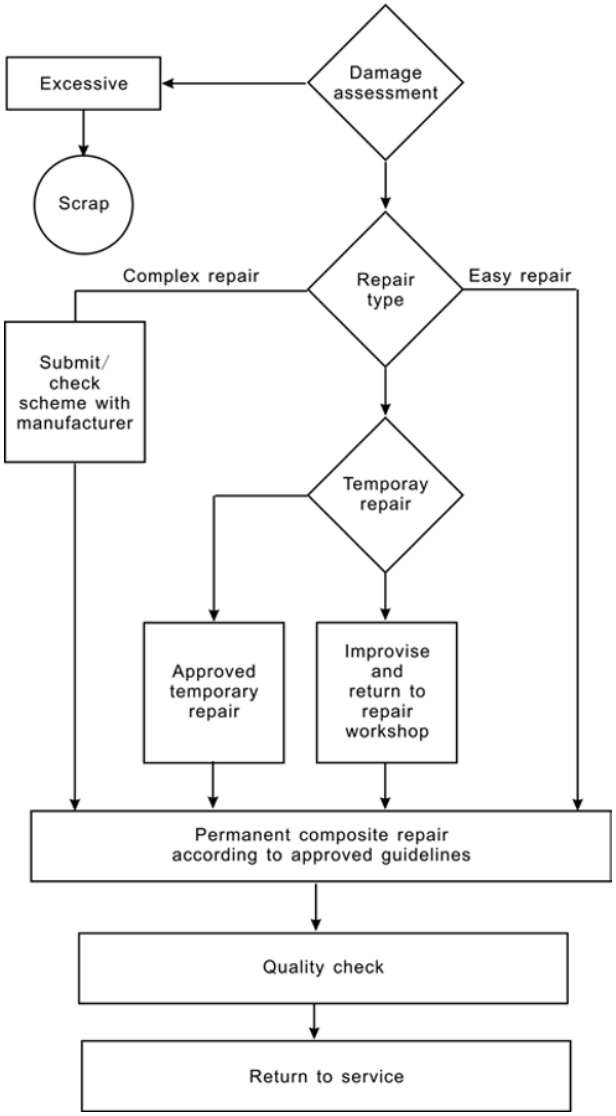

Scheme 1.1 Flow chart of the key stages for thermosetting composite repair.

Most damage to fiber reinforced polymer composites is a result of low velocity (and sometimes high velocity) impact [5]. In metals the energy is dissipated through elastic and plastic deformations, and a good deal of structural integrity is retained. In polymer composites the damage is usually more extensive than that seen on the surface. Typical damage is summarized in the following. (i) Delamination following impact on a monolithic laminate. (ii) Laminate splitting, which does not extend through the full length of the part. Its influence on the mechanical performance depends on the length of split relative to the component thickness. (iii) Heat damage, a local fracture with separation of surface plies. Its effect on the mechanical performance depends on the thickness of the part.

(iv) Dents in a sandwich structure. (v) Puncture damage in a sandwich structure. (vi) Bolt hole damage, which could be elongation of the hole causing laminate splitting, or damage to the upper plies.

Patch repair, a main technique based on adhesive bonding, involves covering or replacing of the damaged portions with a new material [5–7]. It restores the load path weakened or removed by damage or cracking, ideally without significantly changing the original load distribution. Reinforcements or doublers are used to replace lost strength or stiffness, correct design errors, or to improve performance [8]. Since the main purpose of composite repair is to fully support applied loads and to transmit applied stresses across the repaired area, the patch repair materials must overlap, and be adequately bonded to the plies of the original laminate. In this case, the thickness of the original laminate is made up of filler plies and the repair materials are bonded to the surface of the laminate. The advantages of this approach include the fact that it is quick and simple to do, and there is minimum preparation, while the repaired laminate is thicker and heavier than the original and very careful surface preparation is needed for good adhesion. The degree of property recovery is a function of bonding between the patch and the original material, the presence/orientation of reinforcing fibers and patch thickness [6, 9–12].

In addition to patch repair, there are two similar techniques: (i) taper sanded or scarf repair; and (ii) step sanded repair. For the first one, an area around the hole is sanded to expose a section of each ply in the laminate. Sometimes one filler ply is added to produce a flatter surface. Taper is usually in the region of 30–60:1. Comparatively, the repaired version is only marginally thicker than the original. Each repair ply overlaps the ply that it is repairing, so a straighter and stronger load path is obtained. The freshly exposed surfaces help to achieve tight bonds at the interface. With respect to the second technique, the laminate is sanded down so that a flat band of each layer is exposed, producing a stepped finish. Typical steps are 25–50 mm per layer. Nevertheless, it is worth noting that the method needs high skill and is difficult to do.

To conduct bonded external patch repair for structural components, equipment and ancillaries must be employed (Figure 1.2). The vacuum bag is suited to components with thin sections and large sandwich structures. It involves the placing and sealing of a flexible bag over a composite lay-up and evacuating all the air under the bag. The removal of air forces the bag down onto the lay-up with consolidation pressure of 1 atm. The completed assembly, with vacuum still applied, is placed inside an oven with good air circulation, and the composite is produced after a relatively short cycle cure.

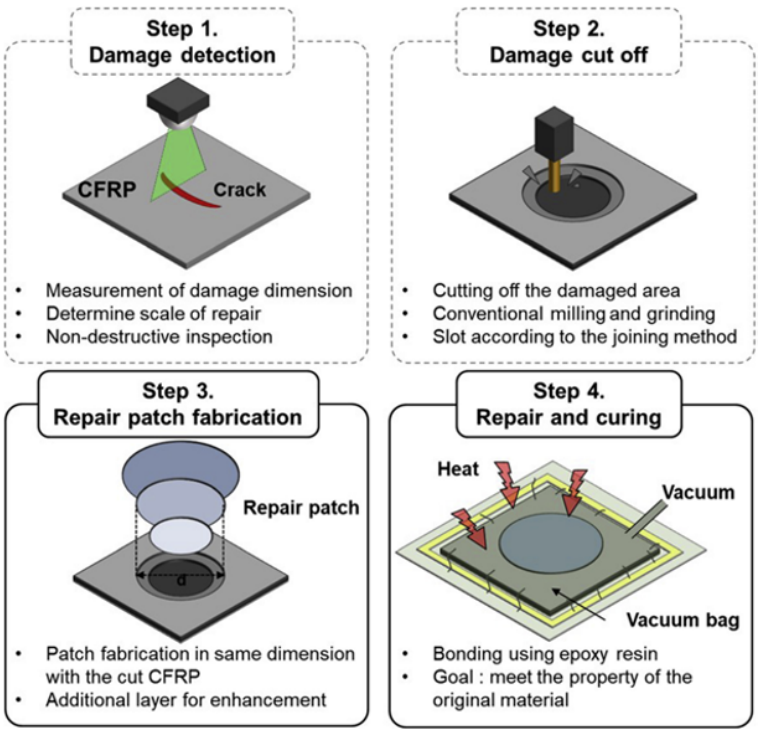

Figure 1.2 Typical repair processes of thermosetting composites represented by carbon fiber reinforcement polymer (CFRP).
Source: Reprinted from Kim et al. [4]. Copyright 2019, with permission from Elsevier.

1.1.2 Fusion Bonding for Healing Thermoplastic Materials

In general, the aforementioned thermosetting adhesive bonding is not directly transferable to thermoplastic polymer-based composite. Fusion bonding, or welding, a long-established technology in the thermoplastic industry, offers an effective way for rejoining fractured surfaces with thermal flowability [13]. Although welding may induce residual stresses if performed without adequate control, it eliminates the stress concentrations created by holes required for mechanical fasteners and so does thermosetting adhesive bonding. In addition, welding reduces processing times and surface preparation requirements [14]. However, the high content of carbon fiber reinforcement in the composites, resulting in high thermal and electrical conductivity, imposes difficulties such as uneven heating, delamination and distortion of the laminates. These problems become more difficult when bonding large components [15]. In addition, as fiber volume fraction increases, the amount of resin available to melt and reconsolidate into a fused joint is reduced and this can affect the welding quality [16].

Fusion bonding techniques can be classified according to the technology used for introducing heat [13, 16] (Scheme 1.2), namely bulk heating (co-consolidation, hot melt adhesives, and dual resin bonding), frictional heating (spin welding, vibration welding, and ultrasonic welding), electromagnetic heating (induction welding, microwave heating, dielectric heating, and resistance welding), and two-stage techniques (hot plate welding, hot gas welding, and radiant welding).

Bulk heating techniques such as autoclaving, compression molding or diaphragm forming are available for performing co-consolidation [17]. Co-consolidation is an ideal joining method as no weight is added to the final structure, no foreign material is introduced at the bond line, essentially no surface preparation is required, and the bond strength is potentially equal to that of the parent laminate. However, the entire part is brought to the melt temperature, and this generally implies the need for complex tooling to maintain pressure on the entire part and to prevent de-consolidation. Hot melt thermoplastic adhesive films may be inserted at the bond line to improve filling of parts mismatch. Inserting of an amorphous polymer interlayer proved to reduce the scatter of strength [18], which widens the processing window. The dual resin bonding, or amorphous bonding, involves co-molding an amorphous thermoplastic film to a semi-crystalline thermoplastic matrix laminate prior to bonding [19]. During the joining step, the amorphous polyetherimide (PEI) film can be fused at a temperature above its glass transition; below the melting temperature of the semi-crystalline polyether ether ketone (PEEK) polymer; avoiding any deterioration of the bonded structure [20].

Spin welding and vibration welding have been extensively used in the plastics industry but are less appropriate to joining thermoplastic composites as the motion of the substrates relative to one another may cause deterioration

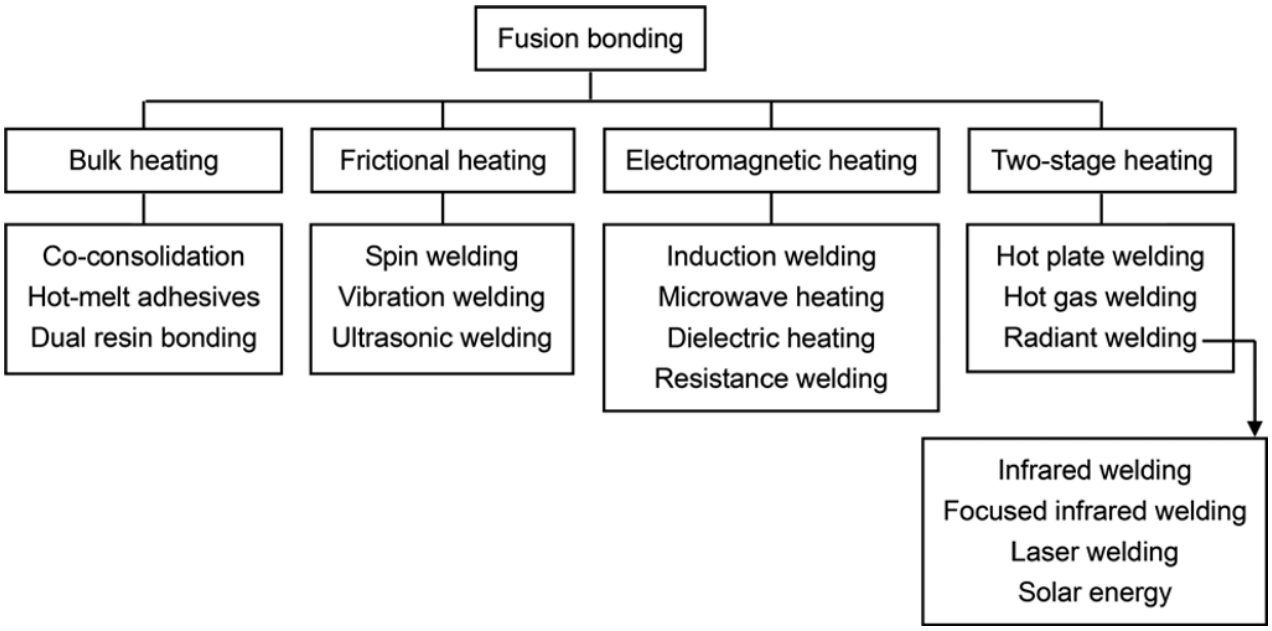

Scheme 1.2 Fusion bonding techniques. *Source:* Reprinted from Ageorges et al. [13]. Copyright 2001, with permission from Elsevier.

of the microstructure, such as fiber breaking. The process was however investigated for joining carbon fiber/PEEK [16] and glass fiber/polypropylene (PP) [21] systems. Microwave and dielectric welding are available for joining thermoplastics [22] but the fact that heating occurs volumetrically and that multilayer composites are excellent shields in the microwave range [23] make these techniques unsuitable for the welding of thermoplastic composites particularly when they are reinforced by carbon fibers.

Ultrasonic welding [24], induction welding [25], and resistance welding [26] are the three most promising fusion bonding techniques. Only the welding interface is brought to the melt temperature, and the impact on the rest of the structure is minimized. Welding times are very short. Large-scale welding may be performed through sequential or scanning approaches, and on-line monitoring of the consolidation is possible.

In two-stage techniques the heating device needs to be removed from between the substrate surfaces between the stages of heating and forging. This aspect involves limitations on size of the component since the whole welding surface must be heated in a single step [27]. Heating times are normally long as they rely on the low thermal conduction of heat through the polymer. Between the heating and forging steps, surface temperature drops and the region experiencing the maximum temperature is located below the skin of the laminate. The high pressure required to consolidate the bond line may cause warpage/flow in the higher temperature inner region [22].

1.1.3 Bioinspired Self-Healing

Although the repair strategies discussed in the previous sections have demonstrated their capability of recovering the load-bearing property of polymers and polymer composites, the complicated procedures typically represented by Figure 1.2 show that they are time consuming and cost ineffective, not including the losses resulting from malfunction of the components. The possible solution of this problem lies in early elimination of cracks, so that no macroscopic damage would eventually occur. As the cracks deep inside the materials are difficult to be perceived and to repair, it would be better if the materials have the ability of self-healing like biological systems.

In fact, self-healing is almost universal in nature. Most structures can repair themselves, after undergoing nonfatal trauma or injury [28–33]. Exceptions are teeth and cartilage, which do not possess any significant vascularity. It is also true that brains cannot self-repair; however, other parts of the brain take up the lost functions.

When an injury causes a blood vessel wall to break, for example, platelets are activated. They change shape from round to spiny, stick to the broken vessel wall and each other, and begin to plug the break. They also interact with other blood proteins to form fibrin. Fibrin strands form a net that entraps more platelets and blood cells, producing a clot that plugs the break [34] (Figure 1.3). The blood clotting is factually a protective mechanism that prevents excessive blood from being lost after an injury and prevents bacteria from getting into the wound. Normal clotting takes place within five minutes. For healing of a broken bone, the following processes are conducted in an autonomic way: internal bleeding forming a fibrin clot, development of unorganized fiber mesh, calcification of fibrous cartilage, and conversion of calcification into fibrous bone and lamellar bone. Clearly, the natural healing in living bodies depends on rapid transportation of repair substance to the injured part and reconstruction of the tissues.

Having been inspired by these findings, continuous efforts are now being made to mimic natural materials and to integrate self-healing capability into polymers and polymer composites. A series of healing concepts that offer the ability to restore the mechanical performance of materials have been proposed and successfully applied. The healing mechanisms and methods involved in nature, such as bleeding, blood cells, and blood flow vascular network, were simulated in the form of microcapsules [36], hollow fibers [37],

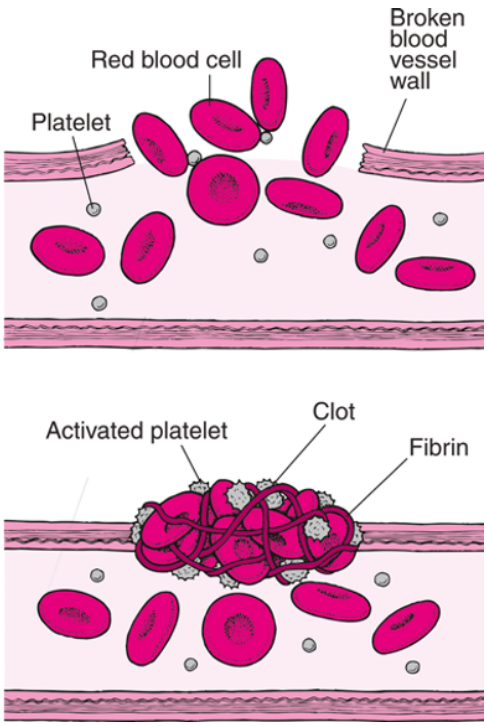

Figure 1.3 Blood clotting in an injured vessel. *Source:* Reprinted from Merck Sharp & Dohme Corp. [35]. Copyright 2020, Merck Sharp & Dohme Corp., a subsidiary of Merck & Co., Inc., Kenilworth, NJ.

nanoparticles [38], and interconnected microchannels [39]. The timescale for realization of self-healing within engineered structures is considerably reduced by a comprehensive exploration and study of the many examples of how the natural world undertakes the process. Biomimicry of the complex integrated microstructures and micromechanisms found in biological organisms offers considerable scope for the improvement in the design of future multifunctional materials [29]. The progress has opened an era of new intelligent materials.

Among the important achievements, the approach using microencapsulation of fluidic healing agent developed by White et al. in 2001 [36] marks a milestone. Since then, the number of scientific publications on self-healing polymers and polymer composites has been significantly increasing (Figure 1.4). The year 2007 was a turning point, meaning an "international race" started, as reflected by both the quantities of published papers and the affiliations of the authors. As of 2015, the number of related reports has multiplied as more and more researchers from different disciplines have become involved. The driving forces may have come from, for example, the rapid consumption of unrenewable crude oil, ecological concerns, advanced application requirements, and the miniaturization and integration of products. A biennial international forum, the International Conference on Self-Healing Materials, has also been established. The first one was held at Noordwijk aan Zee, the Netherlands in 2007. Innovative measures and revolutionary knowledge of the related mechanisms are constantly emerging. It is interesting that the results from different groups complement each other. As a result, the knowledge framework of self-healing polymeric materials is gradually being perfected like a jigsaw puzzle.

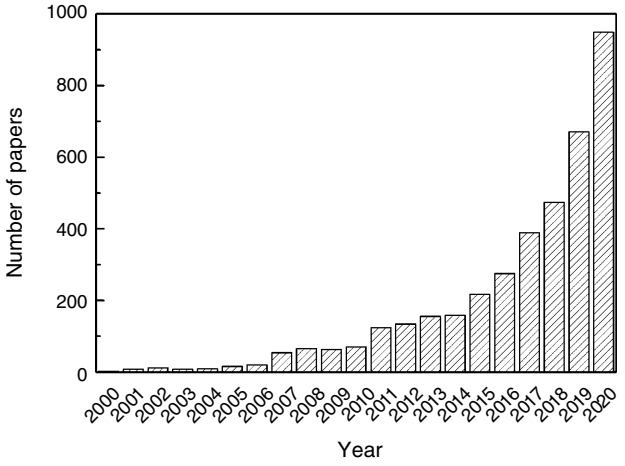

Figure 1.4 Number of research papers on self-healing polymers and polymer composites published between 2000 and 2020 according to the statistics of ISI Web of Knowledge.

One thing that needs to be mentioned is that self-healing has been developed in many laboratories in the world, while a universally accepted definition of this issue is yet to be made. We tend to include a wider scope that considers the following two types according to the ways of healing [40]:

- autonomic (without any intervention);
- non-autonomic (needs intervention/external triggering).

Since this monograph is devoted to the development of new healing chemistry, the focus of the review of the state-of-the-art in the subsequent sections of this chapter will be on the origination of healing capability and the ways of substance supply and energy supply. Accordingly, self-healing polymers and polymer composites will be classified into two categories [41] for the convenience of discussion: (i) intrinsic ones that are able to heal cracks by the polymers themselves without the need of additional healing agent; and (ii) extrinsic in which healing agent has to be intentionally pre-embedded. The prototypes worked out by our group are not analyzed in this chapter but are discussed in Chapters 2–8.

Finally, as viewed from the ultimate outcomes of repair, self-healing would lead to: (i) full-scale restoration; and (ii) functionality restoration. The former recovers the materials to their previous status quo, while the latter recovers the principal function of the materials. A self-healing anti-corrosion coating that operates relying on the embedded inhibitors is a typical example of the latter effect. The authors of this book are more interested in the former.

1.2 Intrinsic Self-Healing

The so-called intrinsic self-healing polymers and polymer composites are based on specific molecular structures and performance of the polymers and polymeric matrices that enable crack healing through inter- and intramacromolecular disconnection and reconnection. Autonomic healing without manual intervention is not available in all cases for the time being. As viewed from the predominant molecular mechanisms involved in the healing processes, the reported achievements mainly consist of three modes: (i) physical interactions; (ii) reversible covalent chemistry; and (iii) supramolecular interactions.

The self-healing based on physical interactions started with crack healing in thermoplastic polymers in the late 1970s. Thermal activation induced macromolecular chain entanglements across the cracked interface, which represents the main healing mechanism. Wool et al. systematically studied the theory involved [42, 43]. They pointed out that the healing process goes through five phases: (i) surface rearrangement, which affects initial diffusion function and

topological feature; (ii) surface approach, related to healing patterns; (iii) wetting; (iv) diffusion, the main factor that controls recovery of mechanical properties; and (v) randomization, ensuring disappearance of the cracking interface. In addition, Kim and Wool [44] proposed a microscopic model for the last two phases on the basis of the reptation model that describes longitudinal chain diffusion responsible for crack healing.

On the other hand, thermomechanical healing proves to be valid for some specific polymers, such as ionomers. An ionomer is a copolymer that comprises repeat units of both electrically neutral repeating units and a fraction of ionized units (usually no more than 15%). With a rise in temperature, the polymer exhibits an order-to-disorder transition as a result of which the ionic clusters, although persisting, lose order and strength. As the temperature is further increased, the semi-crystalline polymer matrix melts, even though the disordered clusters remain and continue to provide increased melt strength [45]. These transformations play a vital role in the self-healing process immediately after impact. When the thermal energy of impact dissipates, the aforementioned reversibility ensures rapid solidification while reordering of the ionic clusters and physical cross-links follows more slowly. The works by Fall [46] and Kalista et al. [47–50] have shown the unique self-healing response in poly(ethylene-*co*-methacrylic acid), which is beyond the aforementioned external thermal activation induced melting [51, 52]. These films are able to heal upon ballistic puncture and sawing damage. This occurs through a heat generating frictional process, which heats the polymer to the viscoelastic melt state and provides the ability to rebond and repair damage. In contrast, a low speed friction event fails to produce sufficient thermal energy favorable to healing. Varley and van der Zwaag conducted a careful investigation on the mechanism involved in the ballistic stimulated self-healing process [45].

Hereinafter, self-healing driven by reversible covalent chemistry and supramolecular interactions is discussed.

1.2.1 Self-Healing Based on Reversible Covalent Chemistry

Reversible polymers share one property in common – reversibility – either in the polymerization process or in the cross-linking process [53, 54]. Such a feature offers versatile possibilities of repeated healing on a molecular scale. So far, intrinsic self-healing polymers can be classified into two groups in view of the properties to be recovered. One deals with restoration of mechanical properties, while the other concerns regaining non-structural functional properties (such as electrical conductivity, transparency, corrosion resistance, and superhydrophobicity) [55]. In this section, a few typical intrinsic self-healing polymers belonging to the former group are quoted according to the type of reversible covalent reaction involved (Table 1.1).

Reversible covalent reactions include general reversible covalent reactions (e.g. reversible addition, reversible condensation, and reversible redox) and dynamic reversible covalent reactions (e.g. reversible exchange and reversible fission/recombination) (Figure 1.5). The key difference between these two groups of reversible covalent reactions lies in the fact that the types of starting reactants of the forward and backward reactions are different in the case of general reversible covalent reactions. In contrast, the forward and reverse reactions of a dynamic reversible covalent reaction occur under the stimulus of a single triggering factor, without completed dissociation of the reversible covalent bonds. As defined by the characteristics of the reversible reactions, the corresponding healing processes are quite different. That is, the healing driven by general reversible covalent chemistry is conducted in a two-step fashion (e.g. at two temperatures), while that by dynamic reversible covalent chemistry proceeds in a one-step fashion (e.g. at a single temperature). The latter not only simplifies the healing process, but also avoids completely losing the load-bearing capacity and integrity of the materials due to disconnection of the reversible bonds during crack healing.

1.2.1.1 Healing Based on General Reversible Covalent Reactions

Thermally Reversible Cycloaddition

Many reported thermally reversible self-healing polymers are bonded by Diels–Alder (DA) linkages. The healing principle lies in disconnection of DA bonds of a polymer through retro-DA reaction at higher temperature followed by reconnection of the disconnected DA bonds via DA reaction at lower temperature. On account of the randomness of the molecular chains at the crack interface, the broken parts can be sewn up by the successive retro-DA and DA reactions. In 2002, Chen et al. first applied DA cycloaddition between multi-furan and multi-maleimide monomers to construct a thermally remendable cross-linked polymer (Scheme 1.3) [56]. The damaged specimen was treated at 150 °C and then cooled down to room temperature, recovering about 50% fracture toughness, which proved the feasibility of solid state reversible covalent reaction for crack rehabilitation. No catalyst was needed for the entire healing process. To improve solubility of the monomers, the authors synthesized two bismaleimide (BMI) monomers with lower melting points in a later work [57]. Higher healing efficiency was observed for the cross-linked polymer owing to the higher mobility of the dangling chains.

Table 1.1 Typical intrinsic self-healing polymers toward mechanical properties restoration based on reversible covalent chemistry.

Polymer[a]	T_g[b] (°C)	Mechanical strength[c–j]	Failure strain (%)	Healing condition	Mechanism	Healing efficiency (%)	Ref.
DA network	N/A	~150[a]	N/A	150 °C	DA cycloaddition	50% recovery of fracture load	[56]
DA network	N/A	~60[a]	N/A	115 °C, 30 min; 40 °C, 6 h	DA cycloaddition	80% recovery of fracture load	[57]
PEA	−30 (DMA)	25.9[b]	1077	RT, 53 d	DA cycloaddition	Average 45% recovery of strain at break	[58]
PFMES	7.8 (DSC)	1.53 ± 0.3[b]	458 ± 30	RT, 10 d	DA cycloaddition	73.7% of the toughness calculated from the area underneath stress-strain curve	[59]
Epoxy-anhydride	93.5–136.5 (DSC)	8.51–29.1[c]	N/A	110–126 °C, 20 min; 80 °C, 72 h	DA cycloaddition	65.9–96% recovery of critical stress of DCDC test	[60]
PU	N/A	25–46.5[b]	250–450	120–130 °C, 1.5–5 min; 55–60 °C, 24 h	DA cycloaddition	>80% recovery of tensile strength	[61–63]
PU	~60 (DMA)	22[b]	1385	NIR, 0.75 W cm^{-2}, 60 s	DA cycloaddition	96% recovery of tensile strength	[64]
PA	4 (DSC)	~0.25[b]	>300	90 °C, 7 h	DA cycloaddition	85% recovery of tensile strength	[65]
PMMA	N/A	44.3[d]	N/A	>280 nm, 10 min	Cinnamate dimerization	0.1~7.8% recovery of flexural strength	[66]
PU	−7.1, 41.2 (DSC)	2.26[b]	141	254 nm, 1 min; 365 nm, 90 min	Coumarin dimerization	70.2% recovery of tensile strength	[67]
Tetra-coumarins	74.5, 76.3 (DSC)	21.1–25.1[f]	N/A	254 nm, 5.41 J cm^{-2}; 365 nm, 16.66 J cm^{-2}	Coumarin dimerization	90% recovery of Vickers hardness	[68]
Bis-thymines	59.8 (DSC)	18.1[f]	N/A	<240 nm, 10 J cm^{-2}; 302 nm, 12.5 J cm^{-2}	Thymine dimerization	95.6% recovery of Vickers hardness	[69]
Dienes-thiol	−3.5 to −16 (DSC)	1.5–4[b]	N/A	RT, 3 d, 85% humidity	Boronic ester hydrolysis/formation	Complete recovery of tensile strength	[70]
PDMS	65 (DSC)	9.64 ± 0.28[b]	9.72 ± 0.19	70 °C, 12 h, water	Boroxine hydrolysis/formation	Complete recovery of tensile strength	[71]
PPG	14.6	3.9[b]	292	35% humidity, 48 h	Iminoboronate hydrolysis/formation	93% recovery of strain at break	[72]
PPG-PAA	−55 (DSC)	1.7–12.7[b]	182–659	Water, 1 min; RT, 6~18 h	Boroxine hydrolysis/formation	87.3–99% recovery of tensile strength	[73]
P(DA-co-BA)	N/A	4.6 ± 0.2[b]	300 ± 30	RT, 3 d, 75% humidity	Boroxine hydrolysis/formation	96.1% recovery of toughness	[74]
SBR	~−5 (DMA)	1.94 ± 0.18[b]	262 ± 18	80 °C, 24 h	Boronic ester exchange	80% recovery of tensile strength	[75]
PU	41 (DSC)	11	~3	70 °C, overnight	Iminoboronate exchange	Complete recovery of tensile strength	[76]
Epoxy-thiol	−35 (DMA)	~0.5[b]	~70	60 °C, 60 min	Disulfide-thiol exchange	Almost 100% recovery of tensile strength	[77, 78]

Epoxy-amine	−35.5 (DMA)	0.23[b]	113	25 °C, 24 h, air	Disulfide exchange	91% recovery of tensile strength	[79]
PUU	−50.39 (DSC)	0.81 ± 0.05[b]	3100 ± 50	RT, 24 h	Disulfide exchange	97% recovery of strain at break	[80]
PDS	−30 (DMA)	~12[b]	50–160	320–390 nm, 2000 mW cm^{-2}, 5 min	Disulfide exchange	Almost 100% recovery of tensile strength	[81]
VPB	N/A	~3[b]	~400	110 °C, 12 h	Disulfide exchange	75% recovery of tensile strength	[82]
VCR	N/A	~9[b]	~650	120 °C, 5 h	Disulfide exchange	92.0% recovery of apparent shear strength	[83]
PU	29.8 (DMA)	9.66[b]	550	Sunlight, 4 h	Disulfide exchange	92.2% recovery of tensile strength	[84]
PHMA	20 (DSC)	7.57 ± 0.82[b]	276 ± 17	120 °C, 70 kPa, 24 h	Disulfide exchange	85% recovery of tensile strength	[85]
PU	−8.2 (DMA)	6.8[b]	9.23	RT, 2 h	Disulfide exchange	75% recovery of tensile strength	[86]
PU	−50; 12.5–62.5 (DMA)	16.0~25.0[b]	1400–2000	70 °C, 24 h	Disulfide exchange	85.0–89.4% recovery of tensile strength	[87]
Epoxy-anhydride	113 (DMA)	5.24[g]	0.5	160 °C, 1 h	Disulfide exchange	95% recovery of shear strength	[88]
PU	−26.9	1.31[b]	380	0.6 W cm^{-2}, 457 nm blue laser, 35 °C, 30 min	Diselenide exchange	84% recovery of tensile strength	[89]
PU	−39.59 (DSC)	0.161[b]	~140	RT, 12 h	Ditelluride exchange	93.8% recovery of tensile strength	[90]
PA	−21.2 (DMA)	0.19[b]	270	25 °C, 24 h, air	Schiff base exchange	98.1% recovery of tensile strength	[91]
Epoxy-amine	19 (DSC)	27–33[b]	~60	90 °C, 3 h	Schiff base exchange	86.3% recovery of tensile strength	[92]
Epoxy-vanillin	75.7 (DMA)	20.5[b]	12	100 °C, 12 h	Schiff base exchange	93.2% recovery of tensile strength	[93]
PS	125 (DMA)	99.4[c]	N/A	130 °C, 2.5 h, Ar	Alkoxyamine	75.7% recovery of critical stress of DCDC test	[94]
Epoxy-amine	52.2 (DMA)	0.38[e]	N/A	90 °C, 1.5 h, Ar	Alkoxyamine	62.2% recovery of impact strength	[95]
PU	−60 (DMA)	0.2[e]	N/A	15–25 °C, 48 h, air	Alkoxyamine	Over 90% recovery of impact strength	[96]
PU	20.3 (DMA)	6.78[b]	175.2	80 °C, 2.5 h, Ar	Alkoxyamine	70.7% recovery of tensile strength	[97]
Epoxy-thiol	12 (DMA)	~0.25[b]	~55	25 °C, 24 h, air	Alkoxyamine	65.6% recovery of tensile strength	[98]
Acrylate-thiol	27 (DMA)	0.42[b]	266	80 °C, 4 h, air	Alkoxyamine	Almost 100% recovery of tensile strength	[99]
PU/SBS/MWCNTs	N/A	6.63[b]	~300	100 °C, 24 h	Alkoxyamine	81.4% recovery of tensile strength	[100]
PU	−7 (DMA)	~25[b]	~900	100 °C, 24 h	Alkoxyamine	90.1% recovery of tensile strength	[101]
PBA	−50	0.065 ± 0.011[b]	N/A	Swollen in acetonitrile, 330 nm UV, 4 h	Trithiocarbonate	Almost 100% recovery of tensile strength	[102]

(*Continued*)

Table 1.1 (Continued)

Polymer[a]	T_g[b] (°C)	Mechanical strength[c–j]	Failure strain (%)	Healing condition	Mechanism	Healing efficiency (%)	Ref.
PU	−34	0.392 ± 0.196[b]	202 ± 46	Visible light, RT, 24 h	Thiuram disulfide	Average 97.4% recovery of tensile strength	[103]
PU	N/A	~0.08[b]	~500	RT, 24 h, air	Diarylbibenzofuranone unit	98% recovery of strain at break	[104]
PU	−58 (DSC)	~0.8[b]	~800	50 °C, 24 h	Diarylbibenzofuranone unit	Almost 100% recovery of tensile strength	[105]
PBD	N/A	~0.6[b]	~0.9	5–22 °C, 10–30 kPa, 15 min–24 h	Olefin metathesis	Restoring most of the strength	[106]
PCO	N/A	2.85 ± 0.38[b]	345 ± 80	50 °C, 16 h	Boronic ester exchange	Average 94.6% recovery of tensile strength	[107]
PLA	50–57 (DSC)	48–60[b]	4.5–5.5	$Sn(Oct)_2$, 140 °C, 30 min, 4 MPa	Transesterification	Maximum 67% recovery of strain at break and 102% recovery of tensile strength	[108]
Epoxy-acid	~20 (DMA)	~0.6[b]	~0.3	$Zn(Ac)_2$, 160 °C, 2 h	Transesterification	Almost 100% recovery of tensile strength	[109]
PBZ	144 (DMA)	2.88[h]	N/A	$Zn(Ac)_2$, 140 °C, 1 h	Transesterification	99% recovery of storage modulus	[110]
ENR/CABt	−11.3 (DMA)	4.5b	400	150 °C, 3 h	Transesterification	96% recovery of tensile strength	[111]
Epoxy-anhydride	70.3 (DMA)	46.5 ± 2.3[b]	1.95 ± 0.10	150 °C, 1 h	Transesterification	Almost 100% recovery of shear strength	[112]
PU	−52 (DSC)	0.93 ± 0.06[b]	301 ± 12	37 °C, 12 h	Urea bond	Average 87% recovery of strain at break	[113]
PU	−72.9 (DMA)	14.8[b]	1200	RT, 130 h	Oxime-urethane	92% recovery of tensile strength	[114]

[a] CABt, citric acid-modified bentonite; PAA, polyacrylic acid; PBA, poly(n-butyl acrylate); PBZ, polybenzoxazine; PCO, polycyclooctene; PDS, polydisulfide; P(DA-co-BA), poly(dopamine acrylamide-*co*-n-butyl acrylate); PDS, polydisulfide; PFMES, poly(2,5-furandimethylene succinate); PHMA, poly(hexyl methacrylate); PMMA, poly(methyl methacrylate); PPG, polypropylene glycol; PUU, polyurethane urea; SBR, styrene-butadiene rubber; Sn(Oct)2, stannous(II) octoate; VCR, vulcanized chloroprene rubber; VPB, vulcanized polybutadiene; $Zn(Ac)_2$, zinc(II) acetate.
[b] DMA, dynamic mechanical analysis; DSC, dfferential scanning calorimetry.
[c] Compact tension facture load, N.
[d] Tensile stress, MPa.
[e] Critical stress measured by double cleavage drilled compression (DCDC) test, MPa.
[f] Flexural strength, MPa.
[g] Impact strength, kJ m^{-2}.
[h] Vickers hardness, Hv.
[i] Shear strength, MPa.
[j] Storage modulus, GPa.

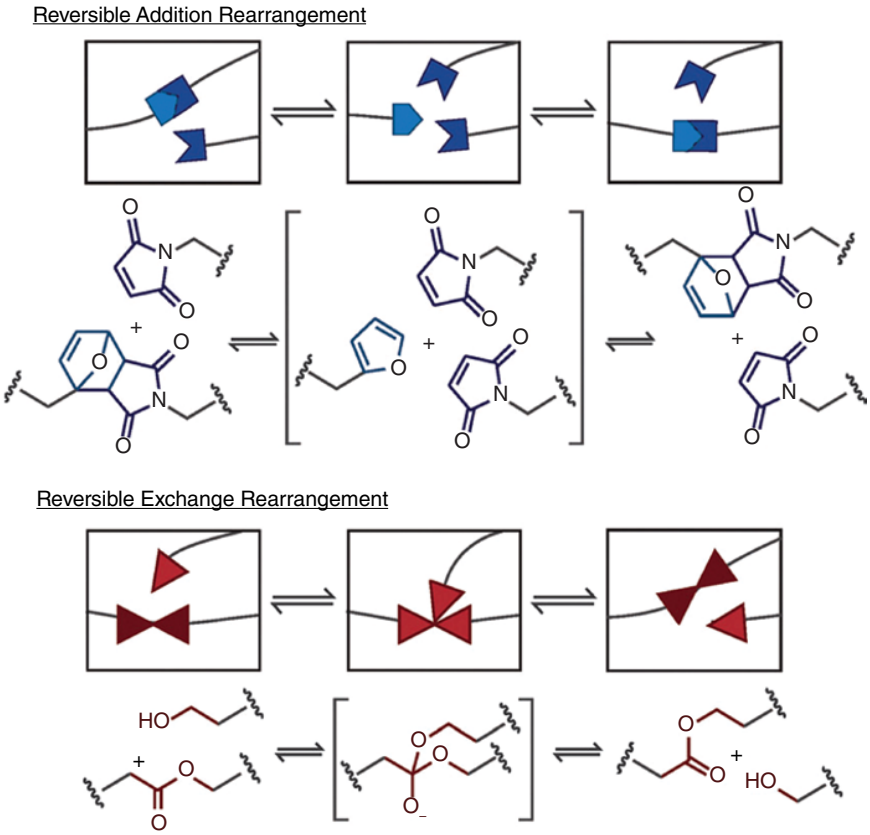

Figure 1.5 Connectivity transition difference for the reversible addition (top) and reversible exchange (bottom) cross-linking reactions. Based on these differences in connectivity, it is clear that both the equilibrium state of these two reactions as well as the dynamic exchange, i.e. the kinetics, between the various states are important. *Source:* Reprinted from Kloxin and Bowman [54]. Copyright 2013, with permission from the Royal Society of Chemistry.

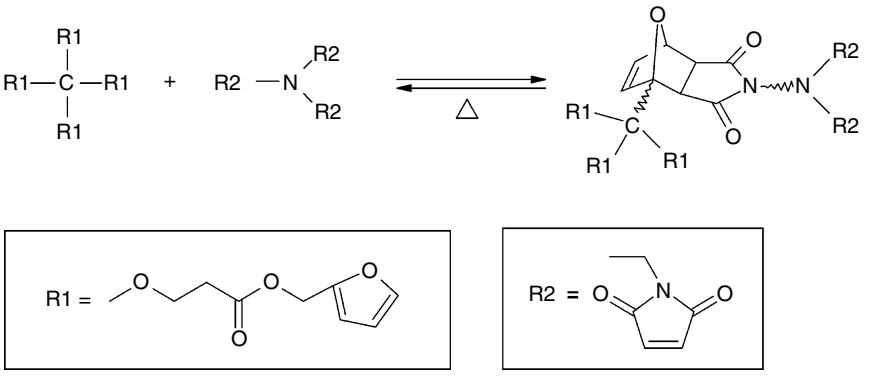

Scheme 1.3 Thermally reversible cross-linking based on Diels–Alder reaction. *Source:* Chen et al. [56]/Elsevier.

Subsequently, composite panels were prepared by sandwiching the DA monomers between carbon fiber fabric layers [115]. Microcracks that were induced on the resin-rich surface of the composites disappeared after treatment at 180 °C for one hour as a result of resistance heating. The experiments demonstrated the self-healing ability of the remendable polymers in both bulk form and fiber composites. Owing to the fast kinetic rate of the reaction of the polymer constituents, which requires a fast injection of the healable resin into the carbon fiber perform, a modified resin transfer mold (RTM) technique was developed accordingly [116]. Besides, Plaisted et al. proposed the concept of multifunctional composites [117], in which the cross-linked polymer from multi-furan and multi-maleimide [56]

serves as the matrix, arrays of straight copper wires and copper coils as the conductive electromagnetic scattering elements, and synthetic fibers as the reinforcement. The scattering elements provide controlled electromagnetic response for tasks such as tuning the dielectric constant and filtering radio frequency radiation. Internal damage, in the form of polymer matrix cracking, may be repaired when heat is applied through the metallic wires. In the meantime, Kwok and Hahn carefully studied the influential factors when using carbon fibers as a resistive heating network for activating the self-healing function [118]. Various electrode methods were tested in an attempt to reduce the contact resistance that caused localized heating around the electrode. In addition, Park et al. confirmed multiple healing and shape memory effects of the composites after electrical resistive heating [119].

Afterwards, Liu and co-workers prepared a self-healable DA bond cross-linked epoxy and high toughness polyamide [41, 120–122], respectively. When the scratched epoxy surface was thermally treated at 120 °C for 20 minutes and at 50 °C for 24 hours, the fissure completely disappeared. However, the cracks on the polyamide film were only partly healed even when the healing time was as long as five days due to the low mobility of polyamide chains. The result showed that the healing behavior was diffusion-controlled [123].

Kavitha and Singha applied click chemistry to make poly(methyl acrylate) (PMA) bearing reactive furfuryl functionality, which was then reacted with BMI to form cross-linked poly(furfuryl methacrylate)-bismaleimide (PFM-BMI) [124]. DA bonds acted as the cross-linking sites, so that the polymer can be de-cross-linked through the retro-DA reaction. Accordingly, a complete notch (knife-cut) recovery to regain the original structure was detected by scanning electron microscopy (SEM) on PFM-BMI film after treatment at 120 °C for four hours.

Murphy et al. simplified the dual monomer route for the synthesis of remendable polymers from DA adducts by replacing the furan-maleimide pair with a single monomer that contained a dicyclopentadiene core unit [125]. The new single-component remendable polymer system utilized the dicyclopentadiene moiety as both diene and dienophile in the thermally reversible DA cycloaddition reaction. Additionally, the Staudinger cross-linking of the dienophilic DA dimer adduct double bond of the growing polymer chains was found to be the key to the strength of the materials. Fracture tests showed that the healing treatment of 120 °C for 20 hours in an argon atmosphere led to an average 46% healing efficiency. Similarly, thermally remendable composites with a dicyclopentadiene-based polymer as the matrix and graphite fibers as the reinforcements were also fabricated [126]. Since the graphite fibers can act as electrical conductors to provide the necessary heat to the polymer, resistance heating was used to stimulate the healing. It was found that microcracks can be healed within minutes at temperatures ranging from 70 to 100 °C.

Syrett et al. used DA chemistry to synthesize polymerization initiators and a dimethacrylic cross-linker that leads to cleavage and reformation required by self-healing [127]. The linker exhibited cleavage properties with 50% reformation occurring upon the reheating cycle. Linear and star methyl methacrylate polymers bearing DA adducts within their macromolecular backbone prepared via living radical polymerization were also preliminarily evaluated to check their ability to cleave and reform under external thermal stimuli.

Cheng et al. [128] extended DA chemistry to organic/inorganic hybrid materials with polyphosphazenes as matrices. Crack healing was performed by DA de-cross-linking at 120 °C for two hours and re-cross-linking at 60 °C for 3~5 days. The authors suggested that appropriate content of the pendant furan moieties and density of DA cross-links were important for achieving better healing effect. Xu et al. [129] reported a stiff and transparent polyhedral oligomeric silsesquioxane-based nanocomposite with crack-healing ability due to the thermally reversible reaction of furan and maleimide moieties. Lee et al. [130] prepared graphene nanoplate (GNP)/polyurethane (PU) nanocomposites via bulk in-situ DA reaction between GNP and furfuryl side chains of PU. The thermally self-healing capability was confirmed by the disappearance of scratch at 110 °C through DA reaction at the interface. Moreover, DA cross-linked bulk polymers with crack healability, such as triple-shape memory poly(*p*-dioxanone)-poly(tetramethylene oxide) (PPDO-PTMEG) co-network [131] and novolac epoxy [132], were also synthesized. These works only assessed the crack-healing ability qualitatively.

In the works by Du et al. [61–63], linear and cross-linked PUs containing DA bonds were developed. The thermally remendable PU displayed tensile strengths ranging from about 25 to 46.5 MPa, and the corresponding healing efficiency could reach more than 80% for the first time. Multiple healing was allowed with gradual decrease in efficiency. Due to the poor heat resistance of PU, thermal treatment at elevated temperature had to result in dissociation of hydrogen bonds and deterioration of mechanical properties [133], which would no doubt affect the healing efficiency.

Thermal reversibility can also be imparted to rubbers. Chen and Jiao used diglycidyl dicyclopentadienedicarboxylic acid ester (DGDCA) as a cross-linking monomer in alkyl aluminum system catalyzed copolymerization with epoxide monomers such as epichlorohydrin (ECH) [134].

The resultant polyether thermoplastic elastomer can be molded into sheets at 215 °C. When the opposite parts of a broken specimen were joined together, the crack became invisible under certain conditions. It means that de-cross-linking of the cross-linked copolymer occurred at elevated temperature, leading to melting and plastic flow. When the material was cooled down, the DA cycloaddition between the side group cyclopentadiene rings reconstructed the elastic cross-linking networks.

Watanabe and Yoshie developed network polymers with recyclability using telechelic prepolymers with reversible reactivity [135]. On the basis of the research, they produced an elastomer from bisfuranic terminated poly(ethylene adipate) (PEA) and tris-maleimide through DA reaction at 60 °C [136]. The resultant polymer, PEAF2M3, possessed a glass transition temperature (T_g) of −34 °C, and can be de-cross-linked by retro-DA reaction at 145 °C for 20 minutes. When a film sample was cut into two pieces and the cut surfaces were kept in contact with each other at 60 °C, rejoining of the cut pieces was observed. This mending was believed to be induced by the following three mechanisms. (i) The reversible cross-linking reaction bridged the cut surfaces. At the cut front, the weak DA adducts were selectively dissociated sacrificially to release the stress to protect the chemical structure of the prepolymer and the linker against the scission or degradation. (ii) Exchange of the maleimide (furan) group in a DA adduct with that in another DA adduct. (iii) Entanglement of dangling chains.

Generally, a fast dynamic exchange rate not only means quick healing of polymer materials, but also rapid creep. To overcome this limitation, Konkolewicz et al. [65] explored the cross-linked acrylate polymer containing both multiple hydrogen bond (weak but fast) and DA linkage (strong but slow), which showed different self-healing behaviors and mechanisms depending on temperature. At room temperature, the exchange of dynamic hydrogen bond allowed for recovering 50% of strain at break within seven hours, while at elevated temperature (e.g. 90 °C), the combination of physical hydrogen bond and DA linkage could recover the majority of its initial mechanical property (90% of strain at break).

Although most of the DA healing requires heating assistance, several systems that possess self-healing ability at room temperature have been developed. Early in 2009, Reutenauer et al. proposed such a DA cross-linked polymer despite the fact that quantitative characterization of healing efficiency was not available [137]. It involved fulvenes as the dienes and bis(dicyanofumarates) or bis(tricyanoeth ylenecarboxylates) as the dienophiles, which was different from the conventional DA chemistry between furan and maleimide. Repairing of the elastomer film was demonstrated by lapping followed by pressing to ensure microscopic contact, and the overlapping area was unable to separate by elongating. Then, Yoshie et al. [58] reported a DA cross-linked polyester, which allowed for autonomous mending of cracks at room temperature based on DA reaction between anthracene and maleimide. The average recovery due to healing at room temperature for 53 days was 17% and 45% in terms of tensile strength and elongation at break, respectively. By increasing the healing temperature to 100 °C, a better recovery was observed after seven days. The healing efficiencies reached 45% and 79%, respectively. Compared with the DA system from the furan-maleimide pair, the DA adduct between anthracene and maleimide is a potential replacement for designing self-healing polymers with high thermal stability, despite the fact that the healing time was obviously longer and the healing efficiency needed to be improved. Similarly, the authors also developed bio-based polymers from bis(hydroxymethyl)furan, which could undergo room temperature self-healing at bulk or with the aid of BMI solutions [59]. Because the kinetic rate and mobility of macromolecular chain segments decrease with decreasing temperature, however, the DA reaction rate has to be suppressed at ambient temperature. Consequently, healing efficiencies of the above polymers were not promising.

Recently, taking advantage of the photothermal effect of polydopamine particles (PDAPs) and the reversible properties of DA linkages, PU/PDAP composites with near-infrared (NIR) triggered shape memory and self-healing properties were fabricated by Xia et al. [64] Typically, the composites (1 wt% PDAPs with 220 nm diameter) were deformed at 65 °C and then cut, followed by irradiation with NIR light (0.75 W cm^{-2}) for 60 seconds to achieve 96% recovery of mechanical strength. The crack was immediately closed in the presence of NIR light due to its shape memory function and healed after the crack closure through DA reaction. The healing efficiency of the broken sample with heating assistance (110 °C, 1 hours; 80 °C, 24 hours) was only 76%.

On the whole, the DA reaction driven self-healing has to be carried out in a two-step fashion as a result of successive retro-DA and DA reactions. During the first stage of healing (i.e. retro-DA reaction/de-cross-linking), creep deformation or even collapse of materials with DA cross-linked linkages often occurs [138, 139] due to molecular cleavage. Evidently, it is a challenge for structural application, where distortion of end-use products is not allowed even if self-healing is proceeding.

In fact, the low viscosity and high mobility of DA cross-linked networks at elevated temperature are ideal for application of self-healing coatings, where load bearing capacity is not the requisite property. Wouters et al. [140] synthesized methacrylate- and epoxy-based DA cross-linked

coatings, which proved to be excellent for scratch healing even if small amounts of coating were scraped off. In comparison with methacrylate-based copolymers obtained from linear precursors bearing furan moieties and BMI, the epoxy networks from DA adduct monomer had much lower initial flow temperature (below 95 °C) and ultimate viscosity (see Chapter 3, Section 3.1 for details). Kötteritzsch et al. [141] described several DA pendant chains containing methacrylate-based copolymers for the development of a one-component coating, which exhibited diverse repair abilities as demonstrated by atomic force microscopy (AFM) and SEM measurements. Various methacrylate co-monomers (e.g. MMA, butyl methacrylate [BMA] and lauryl methacrylate [LMA]) with different chain lengths were used to tune flexibility and mobility of the final copolymers. Due to higher molecular mobility and sub-ambient T_g, the polymer with LMA as co-monomer was able to remend scratches within two minutes at 160 °C or within a much longer time (four hours) at the retro-DA temperature (110 °C). Scheltjens et al. [142, 143] reported a DA cross-linked epoxy coating (thickness = 200 μm) prepared by solution casting, which allowed for flowing above 90 °C. The manual scratches can be completely remended at 130 °C within two minutes. Moreover, Amato et al. [144] used DA linkage-containing soybean-based PU as a two-component automotive topcoat, which displayed remendability of abrasion above 95 °C.

Photoreversible Cycloaddition

In addition to the thermally initiated [4 + 2] cycloaddition, photoinitiated [2 + 2] and [4 + 4] cycloaddition can also be used for the photochemical healing of polymers, as reversion of the cycloaddition to C=C bonds can readily take place in the solid state [145, 146]. Self-healing based on photoreversible reaction is attractive because the use of light is clean, cost-effective, and easily accessible. It is especially suitable for the repair of specific injured regions where the thermal effect is unavailable. In general, ultraviolet (UV) light having shorter wavelength ($\lambda \leq 280$ nm) and that at longer wavelength ($\lambda \geq 280$ nm) are employed for successive photocleavage and photodimerization of the photoresponsive reversible bonds. Due to fast decay of incident light in bulk polymer, however, the cracks deep inside products could not be healed by this method. Therefore, the most promising application of photo-stimulated self-healing lies in coatings and films.

Chung et al. [66] proposed the first example of photochemical crack healing of a rigid and transparent polymer based on cinnamate [2 + 2] photocycloaddition reaction. The material was first cross-linked by UV irradiation at $\lambda > 280$ nm. When it was subjected to impact load, cleavage of the resultant cyclobutane ring occurred due to its low bond strength. Re-irradiation with UV light at $\lambda > 280$ nm allowed recovery of the cross-linked networks within 10 minutes, but the healing efficiency in terms of flexural strength was low. Froimowicz et al. [147] prepared a polyglycerol dendrimer grafted with anthracene groups, which showed photoreversible cross-linking by exposing to 366 and 254 nm UV light. The cross-linked film with an artificial scratch was first irradiated with UV light at 254 nm to regenerate the macromolecular building blocks, and then kept in darkness for overnight to refill the damaged region. Finally, the cross-linked film was recovered by anthracene [4 + 4] cycloaddition under 366 nm UV light. Obviously, the material is somewhat difficult to be used in practice since the de-cross-linking procedure led to complete disintegration of the networks. More recently, UV-triggered self-healing cross-linked polyphosphazenes were explored by Hu et al. [148]. They introduced photoresponsive ethyl 4-aminocinnamate to the main chains of linear polyphosphazenes as pendant groups, which were then exposed to UV irradiation at 365 nm to obtain cross-linked networks. The retro-[2 + 2] cycloaddition reaction under 254 nm UV light and the [2 + 2] cycloaddition reaction under 365 nm UV light resulted in self-healing of surface cutting of the elastomer as revealed by UV–visible spectroscopy and SEM. Polyphosphazenes are known for their unique backbone consisting of alternating phosphorus and nitrogen, and their attractive properties such as heat resistance and flame retardancy. The photo-self-healability undoubtedly adds to their attractiveness.

In the works by Ling et al. [67, 149, 150], photocross-linked PUs containing coumarin in the main chain and side chain, respectively, were synthesized. By taking advantage of the photoreversibility of coumarin, repeatedly self-healing as characterized by restoration of mechanical strength under UV illumination at room temperature was observed. The influence of the soft and hard segments as well as the coumarin moiety content were discussed. It was found that the rubbery domains originating from phase separation were necessary for improving the efficiency of photo-remending. Subsequently, a coumarin-modified tetrafunctional monomer was successfully synthesized and polymerized using irradiation with 365 nm UV light by Saito et al. [68] The self-healing capability of the resultant polymers was first investigated in terms of scratch healing. Meanwhile, two pieces of polymers were partially irradiated with 254 nm UV light to promote the formation of free coumarin units on the surface, and then reconnected by irradiation with 365 nm UV light to achieve recovery of Vickers hardness over 90%. More recently, Abdallh et al. reported a dynamic linear polymer formed by reversible cycloaddition reaction of a thymine unit-containing functional monomer [69]. Irradiation at wavelengths lower

o

$(C_2H_5)_2O{\cdot}BF_3$-loaded sisal 132, 133
OCA. *See* 2-Octylcyanoacrylate (OCA)
2-Octylcyanoacrylate (OCA) 37
Olefin metathesis 20, 47
One-capsule strategy 185, 190
One-step polyol method 234, 303
Optimal dispersion rate 82
Ortho-dichlorobenzene (DCB) 32
Orthographic factorial design 92–94
Oxygen-centered nitroxide radicals 251, 254

p

PAA. *See* poly(acrylic acid) (PAA); Polyacrylic acid (PAA)
PAH. *See* Polyallylamine hydrochloride (PAH)
Patch repair 3
  scarf repair 3
  step sanded repair 3
PBA-*b*-PS. *See* Poly(n-butyl acrylate)-*b*-polystyrene (PBA-*b*-PS)
PBz resin. *See* Polybenzoxazine (PBz) resin
PCL. *See* Poly(ε-caprolactone) (PCL)
PCMS. *See* Poly(4-vinylbenzyl chloride) (PCMS)
PCMS-TEMPO-EOPh 251, 253
PCMS-TEMPO synthesis 252
PDES. *See* Polydiethoxysiloxane (PDES)
PDI. *See* Polydispersity index (PDI)
PDMS. *See* Polydimethylsiloxane (PDMS)
PEA. *See* Poly(ethylene adipate) (PEA)
PEEK polymer. *See* Polyether ether ketone (PEEK) polymer
PEG. *See* poly (ethylene glycol) (PEG)
PEMA. *See* Poly(ethyl methacrylate) (PEMA)
Pentaerythritol tetrakis(3-mercaptopropionate) (PETMP) 39
Performance improvement, self-healing epoxy 78–84
PETI-ATRP. *See* Pickering emulsion templated interfacial atom transfer radical polymerization (PETI-ATRP)
PETMP. *See* Pentaerythritol tetrakis(3-mercaptopropionate) (PETMP); Polythiol (pentaerythritol tetrakis (3-mercaptopropionate) (PETMP)
PFM-BMI. *See* Poly(furfuryl methacrylate)-bismaleimide (PFM-BMI)
Phosphine ($RhH(PPh_3)_4$) 289
Phosphine-catalyzed disulfide metathesis 318, 322
Phosphine salts 292
Photochemical crack healing 14
Photo-cross-linked interpenetrating polymer network 111
Photopolymerization 111
Photopolymerized sodium acrylate 111
Photoresponsive polyurethane (PU-HEDS-400) 298, 300
Photoreversible cycloaddition 14–15
Photosensitive oligomers 111
PHUs. *See* Poly(hydroxy urethane) s (PHUs)
Physical absorption 120
Physical cross-linking network 28
Physical interactions 6–7
Pickering emulsion templated interfacial atom transfer radical polymerization (PETI-ATRP) 38
π-Electron-rich pyrene 29
π–π Stacking interactions 29
PMA. *See* Poly(methyl acrylate) (PMA)
PMF. *See* Poly(melamine-formaldehyde) (PMF)
PMF-walled microcapsules containing mercaptan (PETMP) 68
PMMA. *See* Poly(methyl methacrylate) (PMMA)
PMU. *See* Poly(oxymethylene urea) (PMU)
PMUF. *See* Poly(melamine-urea-formaldehyde) (PMUF)
POA. *See* Poly(oleic acid) (POA)
Polar–nonpolar interface 38
Polar solvents 291
Poly(4-vinylbenzyl chloride) (PCMS) 251
Poly(acrylic acid) (PAA) 30
Poly(ethyl methacrylate) (PEMA) 203
Poly(ethylene adipate) (PEA) 13
Poly (ethylene glycol) (PEG) 29
Poly(ethylene-*co*-methacrylic acid) 7
Poly(melamine-formaldehyde) (PMF) 37, 66, 69, 70, 110, 190–191, 208
Poly(melamine-urea-formaldehyde) (PMUF) 37
Poly(methyl acrylate) (PMA) 13
Poly(methyl methacrylate) (PMMA) 19, 27, 32, 39, 42, 200
Poly(oleic acid) (POA) 26
Poly(oxymethylene urea) (PMU) 215
Poly(phenylene oxide) (PPO) 37
Poly(styrene-methacrylate) (PSMA) 140
Poly(urea-formaldehyde) (PUF) 36, 37, 65, 69, 175, 176
Poly(vinyl alcohol) (PVA) 160, 190, 191
Poly(ε-caprolactone) (PCL) 28, 278
Polyacrylic acid (PAA) 26
Polyallylamine hydrochloride (PAH) 26
Polybenzoxazine (PBz) resin 26
Poly(furfuryl methacrylate)-bismaleimide (PFM-BMI) 12
Poly(styrene-maleic anhydride)-*block*-polystyrene (PSMA-b-PS) block copolymer 39
Poly(n-butyl acrylate)-*b*-polystyrene (PBA-*b*-PS) 28
Polydiethoxysiloxane (PDES) 41, 42
Polydimethyl siloxane (PDMS) 15, 20, 25, 27, 65, 310
Polydispersity index (PDI) 290, 291
Polydopamine particles (PDAPs) 13
Polyether ether ketone (PEEK) polymer 4, 5
Polyethylene glycol 298
Poly(tetramethylene ether) glycol (PTMEG) 28
Polylactide (PLA) vitrimers 18
Polymeric wedge 87
Polymerizable emulsifier (sodium 3-methacryloyloxy-2-hydroxypropane sulfonate (HPMAS)) 111–113, 115–116
Polymerizable monomer 190
Polymerization kinetics 87
Polymerization process 7
Polymers
  alkoxyamine thermal reversibility 251–258
  autonomic crack rehabilitation 64
  carbon-centered radicals in 257
  elastic and plastic deformations 297
  fragile pipelines 64
  liquid resins/solvents 64
Poly(methyl methacrylate)/n-butyl acrylate [p(MMA/nBA)] system 30

Poly(hexyl methacrylate) networks 16
Poly(*p*-dioxanone)-poly(tetramethylene oxide) (PPDO-PTMEG) 12
Polypropylene (PP) tubes 73, 74, 95–99
Poly(hydroxy urethane)s (PHUs) 20
Polysaccharide-based hydrogel 17
Polystyrene (PS) 110, 111
Polystyrene-*block*-polybutadiene-*block*polystyrene (PS-b-PBD-b-PS) 40
Polysulfide diglycidyl ether 289
Polysulfide network 290, 292
  self-healing performance 292
Polytetrafluoroethylene (PTFE) 279, 311
Polythiol (pentaerythritol tetrakis (3-mercaptopropionate) (PETMP) 66–70, 78
Polythiol-loaded microcapsules 84
Polyurethane (PU) 12, 272
Polyurethane urea (PUU) elastomer 16
Polyvinylidene fluoride (PVDF) 303
Porous media 120–122, 189
Post-cross-linking portions 109
PPDO-PTMEG. *See* Poly(*p*-dioxanone)-poly(tetramethylene oxide) (PPDO-PTMEG)
PPO. *See* Poly(phenylene oxide) (PPO)
PP tubes. *See* Polypropylene (PP) tubes
Proton nuclear magnetic resonance (^{1}H-NMR) spectroscopy 198, 203, 227
PS. *See* Polystyrene (PS)
PS-based composites
  GMA-loaded multilayered microcapsules 208–210
  self-healing performance of 210–215
PS-b-PBD-b-PS. *See* Polystyrene-*block*-polybutadiene-*block*polystyrene (PS-b-PBD-b-PS)
Pseudo-plasticity 169
PSMA. *See* Poly(styrene-methacrylate) (PSMA)
PTFE. *See* Polytetrafluoroethylene (PTFE)
PU. *See* Polyurethane (PU)
PUF. *See* Poly(urea-formaldehyde) (PUF)
PU-HEDS-400. *See* Photoresponsive polyurethane (PU-HEDS-400)
Puncture damage 3
PU prepolymers synthesis 278–279
PVA. *See* Poly(vinyl alcohol) (PVA)
PVDF. *See* Polyvinylidene fluoride (PVDF)
Pyrene-modified β-CD (Py-β-CD) 30
2,6-Pyridinedicarboxamide ligands 25
Pyrolysis 70, 162, 193
Pyrolytic performance 193
Py-β-CD. *See* Pyrene-modified β-CD (Py-β-CD)

r

Radical stabilization energy (RSE) 274
RAFT polymerization. *See* Reversible addition-fragmentation chain-transfer (RAFT) polymerization
"Ray cell" structure 33
RCP. *See* Redox cationic polymerization (RCP)
Real-time micro-infrared spectra 142
Redox cationic polymerization (RCP) 110
  advantages of 110
  of GMA 152
Reduced graphene oxide (RGO) nanosheets 31
Remendable polymers 12
Remoldable cross-linked polysulfide 288–297
Resin transfer mold (RTM) technique 11
Resistance welding 5
Retro-DA reactions 229, 230
  enthalpy of 242
  glass transition temperature 244
  thermal remendable polymer 236
Reversible addition-fragmentation chain-transfer (RAFT) polymerization 19, 26
Reversible covalent chemistry 7, 8–9
  hydrolysis-bonding equilibrium 15–16
  photoreversible cycloaddition 14–15
  thermally reversible cycloaddition 7–14
RGO nanosheets. *See* Reduced graphene oxide (RGO) nanosheets
Rhodium catalyst 289
Ring-opening addition reaction 226
Ring-opening metathesis polymerization (ROMP) 39, 41, 163, 190
ROMP. *See* Ring-opening metathesis polymerization (ROMP)
Room temperature curing agent 159
Room-temperature self-healable 288–297
RSE. *See* Radical stabilization energy (RSE)
Rubber
  shape memory 29
  silicone 310
  soft 164
  styrene-butadiene 22
  thermal reversibility 12
  vulcanized 27, 317–326, 328

s

SAM. *See* Scanning acoustic microscopy (SAM)
Scanning acoustic microscopy (SAM) 91
Scanning electron microscopy (SEM) 12, 14, 117, 206, 305
Schiff base-containing chitosan 17, 18
SDBS. *See* Sodium dodecyl benzenesulfonate (SDBS)
Second-order kinetics 237
Self-healing ability 110, 131
  of epoxy composite 147
  polylactide vitrimers 18
  PS composites 210
Self-healing cross-linked polystyrene
  characterization 259–263
  synthesis 258–259
Self-healing epoxy material 33
  characterization 265–270
  with embedded epoxy-loaded microcapsules 164–167
  embedded single-component healant 194–200
  and latent hardener 164–167
  synthesis 264–265
Self-healing functionality 159
  embedded dual encapsulated healant
    crack due to monotonic fracture healing 74–78
    fatigue crack healing 84–90
    impact damage healing 90–95
    performance improvement 78–84

self-pressurized healing system 95–103
Self-healing polymers, 178. *See also* Intrinsic self-healing polymers
bioinspired self-healing 5–6
classification of 6
disulfide bond 288
healant loaded microcapsules 31
healant loaded pipelines 31
physical interactions 6–7
poly(ethylene-*co*-methacrylic acid) 7
polymers and polymer composites 5, 6
polyurethane urea elastomer 16
reversible covalent reaction 7, 8–9
vulcanized rubber reclaiming 317–326
Self-healing specimen 87
crack growth rate 89
crack tip of 146
fatigue life approaches 88
healing efficiency 88, 89
load–displacement curve 150
steady-state stress intensity 89
Self-healing specimen failure 86
Self-healing vascular network 33
Self-healing woven glass fabric 169
Self-pressurized healing system 95–103
SEM. *See* Scanning electron microscopy (SEM)
Semi-crystalline polymer matrix 7, 16
Semi-crystalline thermoplastic matrix 4
SENB tests. *See* Single-edge notched bending (SENB) tests
Shape memory polymers (SMPs) 277
characterization 280–285
synthesis 278–280
Shell wall synthesis 70
Silica-based sol–gel reactions 40
Silica walled microcapsules
$SbF_5{\cdot}HOC_2H_5/HOC_2H_5$ 140
TfOH 146
Silicone elastomer (SR-SH) model 311
Silicon hydrogen bond 263
Siloxane cross-linked polymer 19
Silver nanowires (AgNWs) 302–308, 302–309
Single-capsule system 35
Single-component remendable polymer system 12
Single-edge notched bending (SENB) tests 165, 167
Single-part adhesive 32
Single-walled carbon nanotubes (SWCNTs) 30
Si—O bonds 263
$Si[OSn(n\text{-}C_4H_9)_2OOCCH_3]_4$ (TKAS) 42
Sisal, lignocellulose fiber 120, 122
SMA copolymer. *See* Styrene-maleic anhydride (SMA) copolymer
Small molecule monomers 190
SMANa. *See* Sodium styrene-maleic anhydride copolymer (SMANa)
SMPs. *See* Shape memory polymers (SMPs)
Sodium carbonate solution 67
Sodium dodecyl benzenesulfonate (SDBS) 190, 191
Sodium polyacrylate (PAANa) solution 160
Sodium styrene-maleic anhydride copolymer (SMANa) 66–67, 69, 70, 111, 112, 127, 215, 216
Sol–gel process 22, 140
Solid–liquid transition temperature 73
Soxhlet apparatus 112
Spin welding 4
SR-SH model. *See* Silicone elastomer (SR-SH) model
S—S bonds 289, 291, 293, 296
SS-MTQ. *See* Disulfide bond-containing silicone resin (SS-MTQ)
Stannous(II) octoate ($Sn(Oct)_2$) 18
Steady-state stress intensity 89, 90
Step sanded repair 3
Stick-slip process 77
Stöber chemistry 40
Stress–strain curve starts 168, 169
Styrene 190, 215
molar feeding ratio of 261, 262
Styrene-maleic anhydride (SMA) copolymer 39, 111
Sunlight self-healing cross-linked polyurethane
commercial silicone elastomer 309–317
cross-linked polyurethane 297–302
Supramolecular elastomers 28
Supramolecular interactions
coordination bond (dative bond) 22–26
host–guest inclusion 30–31
hydrogen bonds 27–29
intermolecular forces 29–30
ionic associations 26–27
Supramolecular network 27
Supramolecular polymer 29, 30
Supramolecular polymer gel 31
Surface damage 99
SWCNTs. *See* Single-walled carbon nanotubes (SWCNTs)
Synchronous covalent bond fission 262, 278
Synchronous reversibility 261

t

Tailor-made polymers 200
Tapered double cantilever beam (TDCB) 75–77, 83, 84, 194, 274
epoxy specimens healing efficiency 86
fatigue crack propagation behavior 85
self-healing specimens 89
TBAF. *See* Tetrabutylammonium fluoride (TBAF)
TBP. *See* Tri-*n*-butylphosphine (TBP)
t-CNs. *See* Tunicate cellulose nanocrystals (t-CNs)
TDCB. *See* Tapered double cantilever beam (TDCB)
TDI. *See* Toluene-2,4-diisocyanate (TDI)
TDI-terminated poly(propylene glycol) (PPG-TDI) 38
TEA. *See* Triethanolamine (TEA)
Telechelic prepolymers 13
TEMPO. *See* 2,2,6,6-Tetramethylpiperidine 1-oxyl (TEMPO)
Tensile tests 295
TEOS. *See* Tetraethyl orthosilicate (TEOS)
TEPA. *See* Tetramethylene pentamine (TEPA)
TETA. *See* Triethylene tetramine (TETA)
Tetrabutylammonium bromide (Bu_4NBr) 202
Tetrabutylammonium fluoride (TBAF) 210

Tetraethyl orthosilicate (TEOS) 39, 140, 210, 310
Tetrafunctional thiol 288
Tetrahedral boronic ester 16
Tetrahydrofuran (THF) 202, 228, 251
Tetramethylene pentamine (TEPA) 95, 164, 166, 167, 177, 219
2,2,6,6-Tetramethylpiperidine 1-oxyl (TEMPO) 251
TfOH-loaded silica capsules 146–151
TGA. *See* Thermogravimetric analysis (TGA)
Thermal degradation behaviors 162
Thermally reversible cycloaddition 7–14
Thermal mechanical analysis (TMA) 262
Thermal remendable polymer 236, 238
Thermal reversibility 12, 224, 241
Thermogravimetric analysis (TGA) 176, 193, 267
Thermoplastic polymer matrices 40, 200
Thermoplastic polyurethane (TPU) 16
Thermoplastics 110
  healing approach for 110
  IBH/GMA-loaded microcapsules 151
  $NaBH_4$ particles 151–155
  self-healing PS composites 151–155
  self-healing system 178
Thermoplastic tubing 74
Thermosetting
  boron-containing curing agent encapsulation 120–130
  embedded dual encapsulated healant 135–140
  $SbF_5{\cdot}HOC_2H_5/HOC_2H_5$-loaded silica capsules 140–146
  self-healing functionality 130–135
  silica walled microcapsules
    $SbF_5{\cdot}HOC_2H_5/HOC_2H_5$ 140
    TfOH 146
  TfOH-loaded silica capsules 146–151
  thermoplastics
    IBH/GMA-loaded microcapsules 151
    $NaBH_4$ particles 151–155
    self-healing PS composites 151–155
  ultraviolet irradiation-induced interfacial copolymerization 111–120
Thermosetting adhesive bonding 4
Thermosetting polymers 200
THF. *See* Tetrahydrofuran (THF)
Thick polymer wedge 90
Thick Teflon film 168
Thiol–disulfide exchange reaction 288
Thiuram disulfide (TDS) 19
3D microvascular network 33, 35
Three-dimensional microvascular networks 33–35
TMA. *See* Thermal mechanical analysis (TMA)
TMPMP. *See* Trimethylolpropane tris(3-mercaptopropionate) (TMPMP)
Toluene-2,4-diisocyanate (TDI) 37
TPMD. *See* Knoevenagel condensation product (TPMD)
TPP. *See* Triphenylphosphine (TPP)
TPU. *See* Thermoplastic polyurethane (TPU)
Traditional crack closure concept 87
Transesterification exchange reactions 18–19
Triethanolamine (TEA) 298
Triethylene tetramine (TETA) 130
Trifluoromethanesulfonic acid (TfOH)-epoxy pair 110, 148–149, 289
Trimethylolpropane tris(3-mercaptopropionate) (TMPMP) 29
Tri-*n*-butylphosphine (TBP) 289, 290
  disulfide metathesis 291
  low-molecular-weight disulfides 291
  polysulfide network 292
Triphenylphosphine (PPh_3) 321
Triphenylphosphine (TPP) 79
Trithiocarbonate (TTC) unit 19
T-scan ultrasonic images 181, 183
Tunicate cellulose nanocrystals (t-CNs) 27
"Tweezer-type" receptor units 29
Two-stage techniques 4, 5
Two-step method 234
Typical load–displacement curves 96, 97

u

Ultrasonic non-destructive evaluation technique 95
Ultrasonic welding 5
Ultraviolet (UV) irradiation 111, 112, 113, 118, 119
Ultraviolet (UV) light 14–15, 22, 112
Urea-formaldehyde 37
Urea-formaldehyde resin 160, 161, 164
  colloid theory of 176
Urea-formaldehyde resins 70
2-Ureido-4-pyrimidinone (UPy) 28, 29
UV irradiation. *See* Ultraviolet (UV) irradiation
UV light. *See* Ultraviolet (UV) light

v

van der Waals force 120
Vibration welding 4
4-Vinylbenzyl chloride 251
Vinyl monomers 39
VR-SH specimens 324, 325
V-shaped crack tip 285
Vulcanized rubber reclaiming 317–326

w

Water-insoluble polymer networks 161
Water-soluble methylol urea prepolymer 161
Wide angle X-ray diffraction (WXRD) spectra 274
WXRD spectra. *See* Wide angle X-ray diffraction (WXRD) spectra

x

Xenon lamp light intensity 301

y

Young's modulus of epoxy 169, 177, 180, 306

z

ZDMA. *See* Zinc dimethacrylate (ZDMA)
Zigzag hydrogen-bonded arrays 29, 77
Zinc(II) acetate ($Zn(Ac)_2$) 18, 19
Zinc dimethacrylate (ZDMA) 26
Zinc oxide (ZnO) 26
ZnO. *See* Zinc oxide (ZnO)